Natural Hazards (2020) 101:911–932
https://doi.org/10.1007/s11069-020-03901-4

ORIGINAL PAPER

Evaluating landscape-scale wildfire exposure in northwestern Iran

Roghayeh Jahdi[1] · Michele Salis[2] · Fermin J. Alcasena[3] · Mahdi Arabi[4,5] · Bachisio Arca[2] · Pierpaolo Duce[2]

Received: 7 August 2019 / Accepted: 12 March 2020 / Published online: 20 March 2020

Abstract

We implemented a fine-scale fire modeling approach to assess wildfire exposure in the highly valued resources and assets (HVRAs) of Ardabil Province (18,000 km^2), northwestern Iran. For this purpose, we used the minimum travel time algorithm and simulated 60,000 wildfires under wildfire season most frequent weather scenarios. Wildfire exposure was analyzed on different vegetation types and municipalities using burn probability (BP), conditional flame length (CFL), and fire size (FS) modeling outputs. Also, we obtained the fire potential index (FPI) and source–sink ratio metrics to assess wildfire transmission across the study area. The BP ranged from 0.0003 to 0.013 (mean = 0.0008) and varied substantially among and within the HVRAs of the study area. While the lowest BP values located in broadleaf forests, the highest BP values concentrated on flashy fuel areas, including cereal crops, mountain meadows, and grazed pastures. The average CFL was 0.3 m, with the highest values peaking in cereal crops and wooded pastures located on slopes. FS ranged from about 1–1700 ha, with an average value of 225 ha. Fires ignited in the northern part of the study area resulted in the most significant FS values, due to the large contiguous patches of high fuel loads. High FPI values were associated with large fire ignition areas and anthropic fire occurrence hotspots in the northern and southern parts of the study area. Cereal crops and grazed pastures behaved as relevant wildfire sources of fires exposing rural communities. The results of this study may help support the development of an improved wildfire risk management policy in the study area. The methods from this study could be replicated in neighboring areas and other cultural landscapes of the Middle East, where wildfires pose a threat to human assets and natural values.

Keywords MTT algorithm · Wildfire management · Burn probability · Wildfire risk

✉ Roghayeh Jahdi
roghaye.jahdi@gmail.com

[1] Faculty of Agriculture and Natural Resources, University of Mohaghegh Ardabili, Ardabil, Islamic Republic of Iran

[2] Institute of BioEconomy (CNR IBE), National Research Council of Italy, Sassari, Italy

[3] Department of Agricultural and Forest Engineering, University of Lleida, Lleida, Spain

[4] Shahid Rajaee Teacher Training University, Tehran, Islamic Republic of Iran

[5] University of Southern Queensland (USQ), Toowoomba, QLD, Australia

1 Introduction

Wildfires in forests and grasslands are prevalent throughout Iran, and the vulnerability of these natural ecosystems to fire will likely increase in the future as a result of climate change (Jahdi et al. 2014; Abatzoglou et al. 2018). In fact, every year in the country some 1500 fires burn about 15,000 ha of forest and rangelands (2003–2016) (Data from FRWO personal communication 2016; Andela et al. 2019). Nonetheless, preemptive wildfire management is scarce and the implementation of risk mitigation efforts requires the occurrence of a catastrophic events while decision-making relies on expert criteria. Most previous studies conducted in Iran analyzed the relation between weather conditions and biophysical variables with the forest fire occurrence, hazard, and wildfire risk at various scales using remote sensing data and geographic information systems (Mahdavi et al. 2012; Jafarzadeh et al. 2017; Pahlavani and Bigdeli 2017). Jafarzadeh et al. (2017), for instance, evaluated forest fire risk in the west of Iran using the a priori algorithm and fuzzy *c*-means (FCM) clustering. The results showed strong relationships between wildfire occurrence and multiple variables including distance to urban areas, population density, distance to roads, slope, type of vegetation, temperature, land cover, and distance to farmlands. Adab et al. (2018) applied the ecological niche theory through the maximum entropy (MaxEnt) method to estimate fire hazard potential and the association with different anthropogenic and biophysical conditions, by using different modeling approaches (heuristic, permutation, and jackknife metrics) in northern Iran. However, limited studies explored the contribution of the main causative factors to wildfire exposure in the Hyrcanian and Zagros ecological regions (northwestern Iran) despite the high socioeconomic and natural interest of these sites (Adab et al. 2013; Eskandari et al. 2013; Eskandari and Chuvieco 2015; Jahdi et al. 2015, 2016; Jaafari et al. 2017).

The terms of wildfire hazard, exposure, and risk are related, but not synonymous (Miller and Ager 2013; Scott et al. 2013). Hazard is a physical situation with the potential to cause damage to specific highly valued resources and assets (HVRAs) (Scott 2007), resulting in losses (of value). The hazard in wildland fire is "the potential for loss but does not integrate the likelihood of the event occurring, and fire intensity and crown fire activity are the most widely used metrics" (Miller and Ager 2013). Fire risk is the expectation of loss or benefit to any number of social and ecological values affected by fire (Finney 2005). The risk assessment framework allows assessing the potential risk posed by wildfire to HVRAs across vast landscapes (Scott et al. 2013). On the other hand, exposure describes the spatial juxtaposition of values with fire behavior in terms of likelihood and intensity but does not explicitly describe fire effects on those values (Ager et al. 2012; Miller and Ager 2013; Salis et al. 2013). Quantitative wildfire exposure and risk assessment provide the foundation for cost-effective mitigation of risks and restoration of landscapes and further for monitoring exposure and risk trends through time (Thompson et al. 2013; Dunn et al. 2020).

The variety of wildland fire behavior models with varying inputs, structures, outputs, and intended uses is developed to better understand potential wildfire activity, quantify landscape wildfire exposure and risk, evaluate alternative risk management strategies, and assess the effects of varying environmental conditions on fire behavior (Sullivan 2009a, b, c; Thompson and Calkin 2011; Miller and Ager 2013). These models are typically based on forward rate-of-spread algorithms that were predominantly developed using observations of experimental fires (Duff et al. 2018). Fire growth models can simulate a number of scenarios and have been increasingly used in fire risk assessment in the last decades (Ager et al. 2010, 2014, 2019; Haas et al. 2013; Salis et al. 2016, 2018; Thompson et al.

2016; Alcasena et al. 2016, 2019; Palaiologou et al. 2018, 2019; Parisien et al. 2018). The focus on much of this work has been estimating burn probabilities for an entire landscape given the uncertainty of ignition locations (Ager et al. 2007; Braun et al. 2010). Fundamentally, burn probability modeling attempts to capture spatial variability in fire likelihood and spread potential stemming from variation in possible ignition locations, weather patterns, topography, and fuel conditions (Parisien et al. 2010, 2013; Parks et al. 2012; Salis et al. 2015; Riley and Thompson, 2017).

The minimum travel time (MTT) algorithm is used to conduct fire behavior modeling for estimating fire size, spread direction, fire intensity, and burn probabilities (Finney 2002, 2006). Further, MTT produces burn probabilities by simulating thousands of potential fires that could burn throughout an area, which is an estimate of the likelihood of a pixel burning given a single random ignition under given burn conditions. Several studies have employed FlamMap MTT for quantitative wildland fire risk assessment based on a historical ignition probability grid (Ager et al. 2007, 2010; Kalabokidis et al. 2014; Salis et al. 2013, 2019; Alcasena et al. 2015, 2017). However, fire behavior modeling systems such as FARSITE and FlamMap have only been calibrated to simulate the spread of few fires in Iran (Jahdi et al. 2014, 2015, 2016).

Exposure analyses are a necessary step in risk assessments and typically reveal much of the same spatial patterns without the complexity of predicting fire effects on specific human and ecological values (Fairbrother and Turnley 2005; Ager et al. 2014). In this paper, we assess wildfire exposure to support risk-informed incident decision-making at the landscape scale, fuel level, municipality level, and for a set of fire weather scenarios in Ardabil Province, northwestern Iran. We used a fire simulation modeling approach to assess key wildfire risk causative factors such as burn probability (BP), conditional flame length (CFL), and fire size (FS) in the study area. For that purpose, we used the MTT algorithm and historic fire ignition distributions to model wildfire spread and behavior. The study area mainly experiences fires in pasture and rangelands that impinge upon the sparse forest resources. Although fire frequency, burned area, severity, and vulnerability to wildfires in Ardabil are lower than other Iranian zones, assessing wildfire risk is a primary goal for fire managers and policy-makers, taking into account the severe events that recently affected neighboring areas (e.g., western Guilan in Hyrcanian region). Furthermore, the likely climate change effects could ultimately lead to disrupted fire activity across Ardabil in future years. The results of this study can be used for fuel management planning and management to reduce the risks posed by wildfires and can be replicated in other countries of the region.

2 Materials and methods

2.1 Study area

Ardabil Province is located in northwestern Iran and has an area of about 18,000 km^2, which is about 1% of the total area of Iran (Fig. 1). The population of Ardabil was estimated at about 1,300,000 (2016 census). The study area is limited by the republic of Azerbaijan to the north, Eastern Azerbaijan Province to the west, Zanjan Province to the south, and both Guilan Province and republic of Azerbaijan to the east. Ardabil is the capital of Ardabil Province and is placed in the southwest of the Caspian Sea and between the

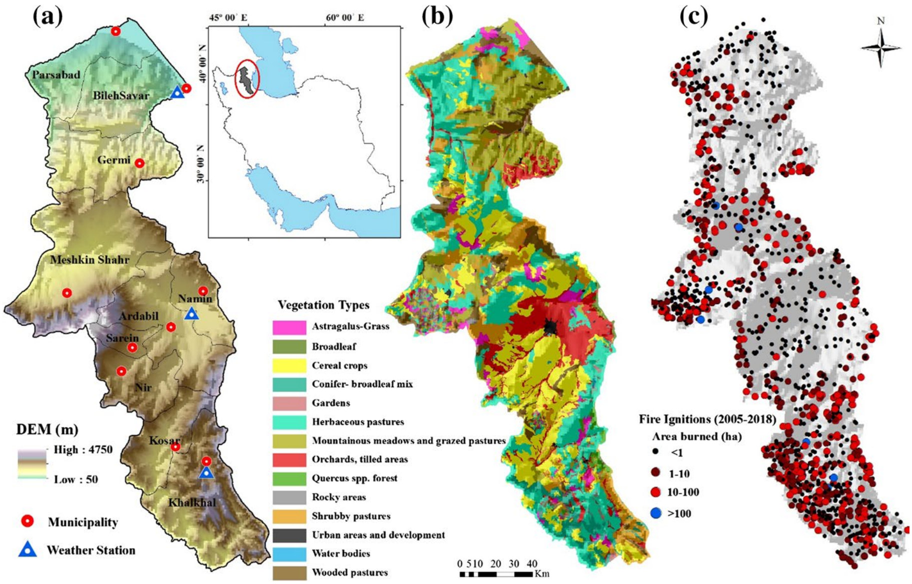

Fig. 1 Maps of the study area (Ardabil Province, northwestern Iran, about 18,000 km^2), with municipality boundaries and elevation as derived by the 30-m DTM (**a**); main vegetation types as derived by the Ardabil Land Use Map of 2016 (**b**); and historical fire ignition locations (June to September; 2005–2018) used for the FlamMap simulations (**c**)

two mountains of Sabalan and Baghro. Parsabad is the biggest city of the province and is situated in northern Ardabil Province. Khalkhal, Meshgin Shahr, and BileSavar are other important cities of the province.

Generally, topography in Ardabil has two main types of plain lands and mountainous farmlands. Elevation values are high, particularly in the southwestern regions of the province. Sabalan Mountain, with a height of 4811 meters, is the third highest peak in Iran. High plains in the north of the province include Moghan plain and mountainous areas with more than 2000 meters high (mainly Sabalan and Talesh Mountains) form the province's natural landscapes. Because of these features, different ecological and economic effects are observed in this province. Northern province in a plain land unit and the semi-steppe vegetative region are associated with vast semi-steppe rangelands, pastures, and dryland agriculture. Southern province in a mountainous land unit and the semi-steppe vegetative region is also covered with shrublands and forestland.

The study area is a complex mosaic of natural and seminatural ecosystems and urban areas (mainly located in hill tops) (Fig. 1b). Natural areas include small forests of Quercus spp. (*Quercus macranthera* Fisch. & C.A.Mey. ex Hohen., *Carpinus orientalis* Mill., *Prunus avium* L., and *Fraxinus excelsior* L.), conifer–broadleaf-mixed forests (*Juniperus excels* M. Bieb., *Pistacia atlantica* Desf var. kurdica Zohary., *Amygdalus scoparia* Spach, and *Crataegus microphylla*), and relatively limited deciduous broadleaf forests (*Corylus avellana* L., *Fagus orientalis* Lipsky, *Quercus castaneifolia* C.A.Mey., and *Carpinus betulus* L.). Seminatural areas are mainly represented by shrublands, perennial grasses, and agricultural (cultivated lands covering cereal crops, orchards, and tilled lands) areas.

The climate of Ardabil Province largely depends on four factors: altitude, latitude, water resources, and air masses. The study area shows large variations in terms of climate

Table 1 Annual and monthly (from June to September, timeframe 2005–2018) average values of mean temperatures (T, °C), maximum temperatures (T_M, °C), minimum temperatures (T_m, °C), and cumulative precipitation (P_P, mm), as well as standard deviation, from three weather stations (Ardabil Airport–BileSavar–Khalkhal) located in the Ardabil Province (Fig. 1a)

Weather station (Elevation (m a.s.l.))	Month	T	T_M	T_m	P_P
Ardabil Airport (1320)	Jun	17.22 ± 1.31	32.78 ± 2.56	3.01 ± 1.40	13.48 ± 11.44
	Jul	18.93 ± 0.98	32.61 ± 2.91	5.83 ± 1.30	3.71 ± 3.62
	Aug	18.92 ± 1.72	34.05 ± .81	4.57 ± 1.24	4.50 ± 3.38
	Sep	15.32 ± 1.09	32.42 ± 2.23	1.46 ± 2.05	12.91 ± 13.03
	Annual Av	9.25 ± 7.80	25.07 ± 7.98	-6.20 ± 10.11	289.29 ± 80.54
BileSavar (100)	Jun	27.13 ± 1.35	36.73 ± 1.78	13.88 ± 1.71	21.05 ± 21.80
	Jul	29.29 ± 1.04	38.55 ± 1.41	17.23 ± 1.10	5.13 ± 7.60
	Aug	29.01 ± 1.70	38.99 ± 1.70	17.15 ± 1.38	7.03 ± 11.67
	Sep	23.88 ± 1.16	34.49 ± 1.49	12.62 ± 1.85	34.08 ± 37.41
	Annual Av	16.59 ± 9.15	28.53 ± 8.01	5.41 ± 8.49	331.36 ± 58.62
Khalkhal (1800)	Jun	17.75 ± 1.26	31.38 ± 2.48	4.08 ± 1.73	17.75 ± 18.51
	Jul	20.28 ± 1.19	33.90 ± 2.23	8.80 ± 2.24	9.01 ± 10.56
	Aug	20.11 ± 1.34	33.95 ± 1.51	6.28 ± 2.23	8.16 ± 8.17
	Sep	16.21 ± 0.99	30.72 ± 1.37	1.72 ± 1.67	10.79 ± 12.86
	Annual Av	9.01 ± 8.52	22.37 ± 9.25	-5.25 ± 9.93	369.82 ± 86.48

(Table 1). The annual mean precipitation in the study area is about 230 mm. Rainfall events are limited in the summer period (33 mm from June to September). Snow events are common during winter. The annual mean temperature is 7.5 °C, while from June to September is 18 °C. The temperature fluctuations in the study area are large: from − 30 °C in January to + 35 °C in June and July.

2.2 Historic wildfire activity

We used the historic fire activity database to determine the duration of the wildfire season and replicate the same ignition locations for wildfires that occurred in Ardabil (Ardabil Natural Resources Department and FRWO, Iran, 2018). We focused on wildfire data from 2005 to 2018 (Fig. 1c). In the last 14 years, on average Ardabil experienced about 97 fires and 640 ha of area burned per year (Fig. 2a). Historically, most fire ignitions have been associated with dry weather conditions and were mostly concentrated from June to September (Fig. 2b). The most of area burned is concentrated in summer, when fuel moisture is lowest, and strong northeast winds are most frequent. The fire events are mainly pasture fires, although these fires can sometimes spread to forest areas. Surface fires are the most common fire type in the study area. The minimum and maximum fire sizes were 0.01 ha and 128 ha, respectively. About 80% of the historical fires in our dataset are less than 10 ha in size: These events affect only about 17% of the total area burned. Fires with burned areas lower than 100 ha account for 72% of the whole burned areas, although they include 19% of the fire number. About 1% of the total number of fires are larger than 100 ha and burnt about 11% of the total area burned. About 95% of the fires have anthropogenic origin. Most fire ignitions relate to human factors such as low distance to transport networks

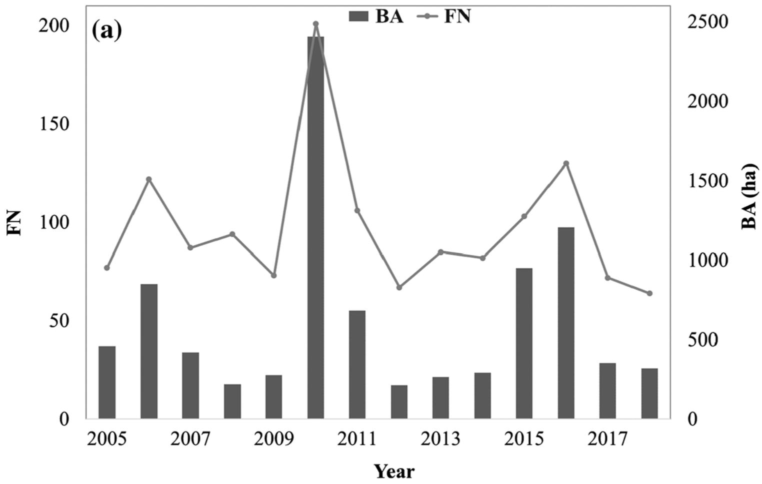

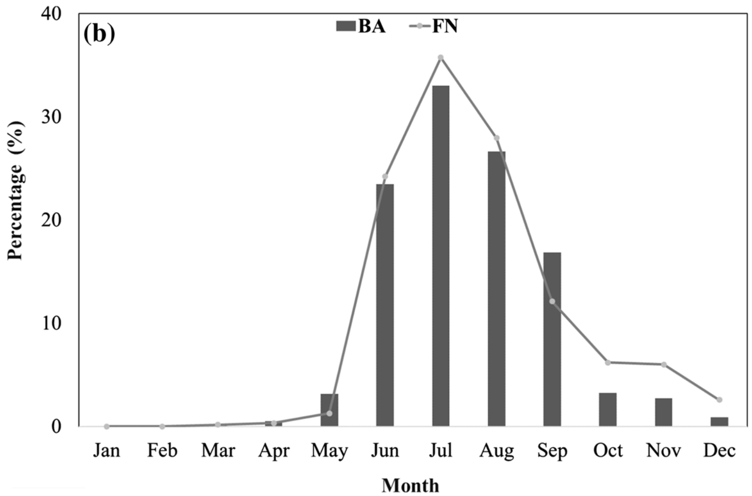

Fig. 2 Fire number (FN) and burned areas (BA) from 2005 to 2018 (**a**), and monthly distribution of FN and BA (**b**) in Ardabil (June to September; 2005–2018). Data from the Ardabil Natural Resources Department and FRWO, Iran, 2018

and urban or recreation areas, the socioeconomic context of the region, factors such as the unemployment rate or variables linked to agricultural activity (farming and land cleaning). Other causes include negligence and arsons related to ecotourism and economic interests. An ignition probability grid (IP) was built from historical ignition locations using inverse distance weighting (ArcMap Spatial Analyst) with a search distance of 5000 m, considering all fire ignition coordinates for the study period (Fig. 1c).

2.3 Input data for wildfire simulations

FlamMap uses inputs related to the landscape, historical weather, and historical fire occurrence to simulate wildfire events. Topography (i.e., elevation, slope, aspect) and fuel model (i.e., surface and canopy fuel maps) input data were assembled in a 100-m resolution landscape file (.LCP), as required by FlamMap (Finney 2006), using ArcFuels 10 (Ager et al. 2011). Topography data were extracted in this study from the digital elevation model (DEM; 30-m resolution). Surface fuels are described by fuel models that characterize dead and live fuel load (by size class), surface-area-to-volume ratio for live and dead fuels, fuelbed depth, moisture of extinction, and heat content. Each fuel model contains information about the fuel bed characteristics and is therefore different per vegetation type (Oswald et al. 2017). Fuel models are difficult to calibrate and are rarely validated with observed fires (Arca et al. 2007; Ager et al. 2011; Salis et al. 2016). Fuel models are extracted from field measurements, selected using photography guides, or obtained from other data sources (Anderson 1982; Scott and Burgan 2005; Arca et al. 2009). Canopy fuels are described by percentage of cover, crown bulk density, crown base height, and average height. In the study area, surface and canopy fuels were obtained from the national land cover dataset (FRWO 2016) by characterizing 14 vegetation types (Fig. 1b) and then assigning a standard fuel model (Table 2, Anderson 1982; Scott and Burgan 2005). The fuel model and canopy cover (percent) maps, along with elevation (m), slope (degrees), and aspect (azimuth), were prepared at a 100-m spatial resolution.

Wildfire spread and behavior depends on conditions that vary on short-time scales such as fire weather and fuel moisture, as well as on fuels, topography, ignition patterns, and suppression response (Calkin et al. 2011; Parisien et al. 2012). We created six fire weather scenarios that were defined by wind speed, wind direction, and frequency (Table 3). These scenarios were based on the most frequent wind directions and average wind speeds observed during the last 14 wildfire seasons (June to September) in the study area. These parameters for the fire modeling were derived from a set of weather stations of the Ardabil Province (Fig. 1a; Table 1), and from the Ardabil Natural Resources Department and FRWO, Iran, 2018. Wind patterns observed in the weather stations for the years 2005–2018 are plotted in Fig. 3. The most common wind directions associated with fires in the study area are from east and northeast, with peaks of average wind speed of about 35 km h^{-1}. The information on live fuel moisture contents (FMC) was derived from other studies with similar vegetation types and condition (Dimitrakopoulos 2002; Arca et al. 2007; Sağlam et al. 2008; Jahdi et al. 2015, 2016). The dead fuel moisture contents were determined by the methods of Rothermel (1983), where the dead fuel moisture content was estimated from weather, topography, vegetation condition data, and fire date (Table 2; Jahdi et al. 2015).

2.4 Wildfire simulation modeling

Modeling approaches were developed to predict and evaluate the simulation accuracy in wildfire spread and behavior. Wildfire simulations were performed by using the minimum travel time (MTT) fire spread algorithm as implemented into FlamMap (Finney 2002). The MTT algorithm replicates fire growth by Huygens' principle where the growth and behavior of the fire edge are a vector or wavefront (Richards 1990; Finney 2002). FlamMap MTT was calibrated with the aim of accurately predicting fires and also validated under different fire environments in USA, Canada, southern Europe, and elsewhere (Ager et al. 2012; Massada et al. 2009; Thompson et al. 2011; Salis et al. 2013, 2015). The algorithm was initially calibrated in the study area by replicating two recent fire perimeters (Khalkhal-Khorosh Rostam fire and Meshgin Shahr-Yeylagh Ghasre Dagh fire, respectively, in the southern and western parts of Ardabil; Table 4). To assess the accuracy of the simulations,

Table 2 Vegetation types derived from the Ardabil Land Use Map of 2016, with the relative incidence in percentage and the respective fuel models used for the wildfire simulations

Vegetation type	Area (km^2)	Incidence (%)	Fuel model	Dead fuel (%)			Live fuel (%)	
				1-h	10-h	100-h	Live herb.	Live woody
Urban areas and development	108.6	0.4	NB1 (Scott and Burgan 2005)	na	na	na	na	na
Orchards, tilled areas	1984.1	8.9	GR1 (Scott and Burgan 2005)	8	9	11	0	40
Water bodies	14.1	0.08	NB8 (Scott and Burgan 2005)	na	na	na	na	na
Rocky areas	18.1	0.13	NB9 (Scott and Burgan 2005)	na	na	na	na	na
Gardens	229.8	1.12	GR1 (Scott and Burgan 2005)	8	9	11	0	40
Cereal crops	3823.6	20.7	GR2 (Scott and Burgan 2005)	8	9	11	0	40
Mountainous meadows and grazed pastures	2591.6	7.35	Mod 1 (Anderson 1982)	8	9	11	0	40
Herbaceous pastures	4996.5	33.73	Mod 2 (Anderson 1982)	8	9	11	0	40
Astragalus–grass	409.3	3.2	GS1 (Scott and Burgan 2005)	9	10	12	0	50
Shrubby pastures	1839.9	11.19	SH2 (Scott and Burgan 2005)	11	12	14	0	70
Wooded pastures	1174.5	6.16	SH5 (Scott and Burgan 2005)	11	12	14	0	70
Broadleaf forest	55.3	0.72	TL6 (Scott and Burgan 2005)	11	12	14	0	80
Conifer–broadleaf mix	437.8	5.36	TU1 (Scott and Burgan 2005)	11	12	14	0	80
Quercus spp. forests	107.1	0.96	TU3 (Scott and Burgan 2005)	11	12	14	0	80

Dead and live fuel moisture contents were associated with recent extreme fire events in the study area and bibliography (Jahdi et al. 2015, 2016), respectively

na not applicable

Table 3 Parameters of the fire weather scenarios used for wildfire simulations

Input data	Description						
Wind scenarios	Scenario number	Sc1	Sc2	Sc3	Sc4	Sc5	Sc6
	Wind direction (°)	40	70	100	130	160	190
	Wind speed (km h^{-1})	13	21	21	30	13	16
	Frequency (%)	18	26	30	9	11	6
Fire ignitions per scenarios	10,000 ignition points considering the historical ignition density grid						

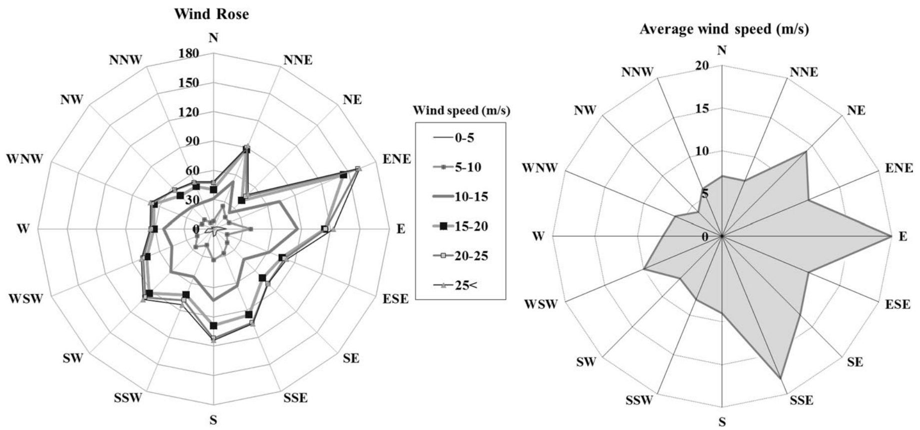

Fig. 3 Wind rose and average wind speed for the Ardabil weather station (June to September, 2005–2018). The axes report the frequency of each wind direction in historical fire events

the Sørensen coefficient (SC; Legendre and Legendre 1998), the Cohen's kappa coefficient (KC; Congalton 1991), and the Overall Accuracy (OA; Congalton and Green 1999) statistics were calculated. The coefficient values range from 0 to 1, with the former value corresponding to a completely failed simulation and the latter indicating a perfect agreement between the fire growth simulations and the reference burnt area perimeter. Wind direction and wind speed were kept constant for the simulations. Consistent with previous findings (Jahdi et al. 2015, 2016), we found a good agreement between actual and simulated fire perimeters (Table 4 and Fig. 4). The simulation statistics of Khalkhal-Khorosh Rostam fire were slightly better compared to the Meshgin Shahr-Yeylagh Ghasre Dagh fire for all indices, even if the difference in terms of accuracy was small. In both fires, the simulation overprediction was noticeable on the flanks (N and NW). The overprediction was especially high in flanking and backing fire spread areas because the fire suppression activities were not considered during simulations.

We simulated 60,000 fires taking into consideration the historical ignition density of the study area for the period 2005–2018. We simulated the fires based on six different wind scenarios and relative percentage of occurrence, as described in Table 3. However, changes in fire management, fuel distribution, and composition in the area, either past or future, have not been factored into our estimates of fire exposure. The simulations were conducted considering constant fuel moisture, wind speed, and wind direction. All

Table 4 Main information of the Khalkhal-Khorosh Rostam and the Meshgin Shahr-Yeylagh Ghasre Dagh wildfires, used to calibrate FlamMap in the study area. The simulation accuracy results are also reported

	Khalkhal-Khorosh Rostam	Meshgin Shahr-Yeylagh Ghasre Dagh
Fire description		
Latitude	37° 21′	38° 17′
Longitude	48° 23′	47° 33′
Elevation (m a.s.l.)	1180	2500
Fire start date (and hour)	July 13, 2016 (12.00)	August 16, 2015 (09.00)
Fire end date (and hour)	July 13, 2016 (20.00)	August 16, 2015 (19.00)
Weather conditions during the fire events		
Temperature (°C)		
Max	29	35
Min	19	21
Relative humidity (%)		
Max	77	55
Min	29	19
Wind speed (km h^{-1})		
Max	22	22
Av	7	4
Average wind direction	S	SW
Precipitation (mm)	0	0
Simulation accuracy		
Observed fire size (ha)	83.5	90.00
Simulate fire size (ha)	149.1	128.80
SC	0.68	0.60
OA	0.95	0.91
KC	0.66	0.55

fire spread simulations were run at 100-m resolution and simulated a fire spread duration of 5 h, which is the common average duration of large historical fires in the study area. Spot probability was set to 0.01 for all the simulations. Fire suppression operations as well as barriers to fire spread were not considered.

The outputs of FlamMap MTT are a burn probability grid, the fire perimeter shapefiles, the flame length probabilities (text file and binary grid), and the fire size list (text file with coordinates and area burned by each fire). Burn probability (BP) for a given pixel is an estimate of the likelihood that the pixel will burn given an ignition within the study area, while considering burn conditions similar to the historical fires (Ager et al. 2012). BP is defined as (1):

$$\mathrm{BP} = F/n \tag{1}$$

where F is the number of times a pixel burns and n is the number of simulated fires (10,000 for every fire weather scenario). Modeled fires burned every pixel at least 10 times and the 99% of the burnable area.

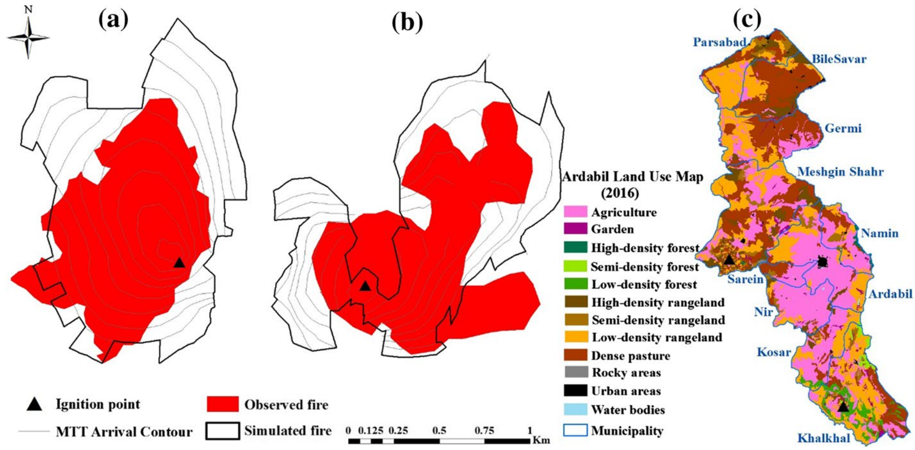

Fig. 4 Comparison between simulated and observed perimeters of the Khalkhal-Khorosh Rostam fire (**a**) and of the Meshgin Shahr-Ghasre Dagh fire (**b**), in Ardabil Province with Ardabil Land Use Map of 2016 (**c**)

The fireline intensity (FI—kW m^{-1}) for a given fuel type and moisture condition can be calculated from the fire spread rate normal to the front (Byram 1959; Catchpole et al. 1982), and then, it is converted to flame length (FL—m) based on Byram's (1959) Eq. (2):

$$\mathrm{FL} = 0.0775(\mathrm{FI})^{0.46} \tag{2}$$

Each pixel has a frequency distribution of flame length generated from multiple fires burning a pixel, which is divided into 20 classes of 0.5-m interval.

2.5 Wildfire exposure analysis

We generated a set of wildfire exposure maps (estimated summary statistics from the output data and the different fire activity metrics) and analyzed them at the landscape scale, fuel level, municipality level, and for each fire weather scenario. We used BP and FL distribution to calculate conditional flame length (CFL; Eq. 3), which is the probability weighted flame length given a fire occurs and is a measure of wildfire hazard (Ager et al. 2010):

$$\mathrm{CFL} = \sum_{i=1}^{20} \left(\frac{\mathrm{BP}_i}{\mathrm{BP}} \right) \left(\mathrm{FL}_i \right) \tag{3}$$

where FL_i is the flame length midpoint of the ith class.

Text files containing the size (FS, ha) and ignition coordinates were used to analyze spatial variation in the size of simulated fires.

The six sets of fire simulation outputs (BP, CFL, and FS) were then weighted according to Table 3 to produce a final map for the study area.

A fire potential index (FPI) was generated based on FS and historical ignition locations as:

$$\mathrm{FPI} = \mathrm{FS} \times \mathrm{IP} \tag{4}$$

where FS is the average fire size for all fires that originated from a given pixel and IP is the historical ignition probability determined from the smoothed map of ignitions. The FPI combines historical ignition probability with simulation outputs on fire size to measure the expected annual area burned for a given pixel. Locations that are characterized by high FPI are likely to have an ignition (e.g., arson) and generate a large fire.

Wildfire transmission among land designations was measured by a source–sink ratio (SSR) of wildfire calculated as the ratio of fire size (FS) generated by an ignition to burn probability:

$$SSR = \log\left(\frac{FS}{BP}\right) \tag{5}$$

The SSR ratio measures the pixel wildfire contribution to the surrounding landscape (in terms of the fire size it produces) relative to the frequency with which it is burned by fires that originated elsewhere or was ignited on the pixel (expressed by the burn probability). In relative terms, pixels that have a high burn probability but do not generate large fires from an ignition are wildfire sinks, and those that generate large fires when an ignition occurs and have low burn probability are wildfire sources (Ager et al. 2012).

3 Results and discussion

3.1 Wildfire exposure at landscape scale

Modeling outputs revealed complex exposure patterns in terms of BP, CFL, and FS across the study area (Fig. 5). The BP results provided a quantitative wildfire likelihood estimate

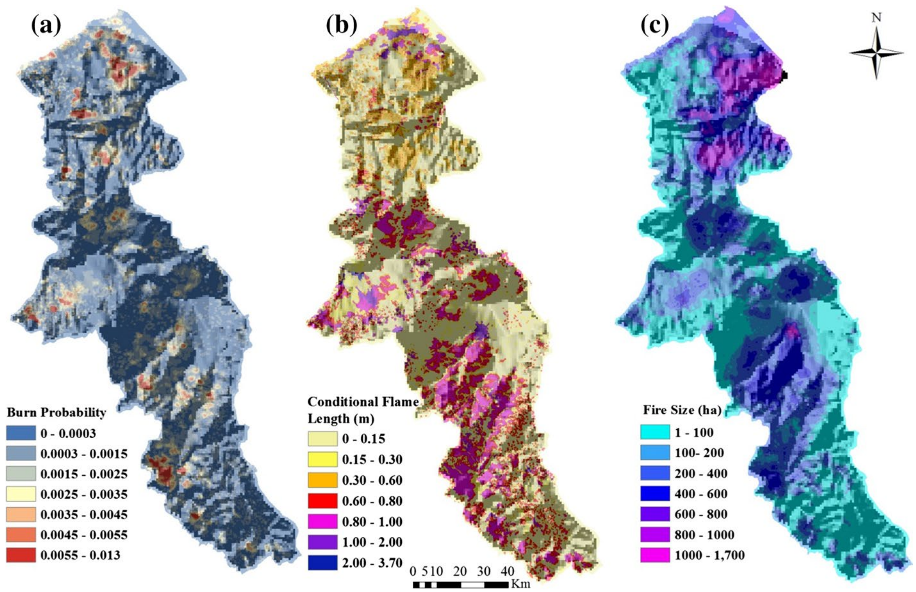

Fig. 5 Burn probability (**a**), conditional flame length (**b**), and fire size (**c**) maps of the study area

based on modeling outputs from thousands of fires while accounting for historic ignition patterns and the dominant weather scenarios occurring during wildfire season (Finney et al. 2011; Haas et al. 2015), rather than focusing on a limited number of fire events that do not capture all the existing variability in terms of fire weather conditions and ignition locations. Therefore, BP modeling outputs represented a major progress in wildfire behavior modeling compared to previous studies conducted in the study area and the neighboring regions (Adab et al. 2013; Jahdi et al. 2015, 2016), where wildfire likelihood was estimated with relatively few predetermined ignition locations (Aghajani et al. 2014; Abdi et al. 2018). Wildfires can spread for very long distances and ignition locations will likely result in a bad predictor of the burned areas for extreme fire events (Miller and Ager 2013). As a result, the BP map revealed which were the areas with a highest exposure in case of a fire ignites under the most frequent fire weather scenarios (Table 4). The BP ranged from 0.0003 to 0.013, and the highest BP values located in the southern and northern portions of the province. This can be related to the wildland fuels continuity and the dry climate conditions. The results confirmed the findings of previous studies conducted in the Zagros ecoregion of Iran, evidencing that wildfires are a recurring phenomenon in this area during the dry season that typically extends from July to August (Jaafari et al. 2019). In the northern part, many of these wildfires are caused by agricultural activities, where the fire is culturally used by local farmers and shepherds to remove post-harvesting remains in cereal crops and clear the grazing areas. The result is consistent with observations in northern Iran where the highest fire likelihood is related to land cover types associated with agricultural activities, thus indicating a strong influence of human activities in fire occurrence in the region (Adab et al. 2018). This burn pattern was also found in other Mediterranean cultural landscapes, where the highest BP values were obtained for cereal crops and herbaceous pastures (Alcasena et al. 2015, 2017; Salis et al. 2018). The highest BP values were associated with the frequent northeast and east wind directions (Sc2 and Sc3). The low BP areas of the landscape correspond to areas with low spread rates, large non-burnable areas, and a low historical ignition probability (Fig. 5), as we saw in the central area of the province. On the other hand, the few forest fuels such as broadleaved forests showed low BP values mostly due to reduced biomass loads in the understory. The low BP values in forest lands of central Ardabil are explained by the intensive management activities including extensive livestock grazing in rangelands and forest thinning for firewood (Naghipour et al. 2015; Faraji et al. 2019). Dormant-season grazing has been suggested as a rangeland fuel treatment, but its effects on fire characteristics are generally unknown (Davies et al. 2015).

The highest fire intensity values (CFL > 1 m) located in small areas of the northern part are mostly covered by shrubby fuels, as well as central-southern part of the study area covered by cereal crops and wooded pastures characterized by high fuel load and height. These results agree with observed wildfire behavior during the largest fire events originating in dryland croplands in the study area (Ardabil Natural Resources Department, Iran, 2018). Agricultural waste field combustion is one important type of anthropogenic biomass burning, especially in the developing countries, in which simultaneous combustion over extended areas can usually facilitate agricultural fire (agri-fire), and then, related emissions cause serious local or regional air pollution during harvesting seasons (Zha et al. 2013), while most of the central-east parts of the study area (i.e., Ardabil municipality) has moderate values (0.15–1 m) and the rest of the area has low values (up to 0.15 m). Low CFL values predominate in the eastern and northern parts of the province. Broadleaf (*Corylus avellana* L., *Fagus orientalis* Lipsky, *Quercus castaneifolia* C.A.Mey., and *Carpinus betulus* L.) forests showed the lowest values (< 0.1 m) (Fig. 5) due to the low fuel load in these fuel types.

FS tends to be much greater in the northern Ardabil because dense grassland and pastures facilitate fire spread. The simulated FS ranged from 1 to 1700 ha. Despite the northern part of the study area presented the largest fires over 800 ha (Fig. 5), the areas with the most common occurrence of large fires (400–800 ha) located in the central and southern parts. Large wildfires in these provincial areas have historically been observed. For example, a wildfire burnt over 200 hectares in rangelands of Khoresh Rostam division in Khalkhal municipality, southern Ardabil on July 13, 2016. Many land use systems in these areas including herbaceous and shrubby pastures are vulnerable to wildfires, and flame length values above 3 m would cause substantial losses (Alcasena et al. 2016). By contrast, the fires were smaller in the eastern part (< 100 ha). These areas were generally characterized by fragmented cultural landscapes with a composition of burnable and non-burnable fuels where intensive human management activities preserved the typical land use land cover mosaic existing in many Mediterranean areas (Fernandes et al. 2012; Mallinis et al. 2016). The discontinuity of fuels in the landscape can produce substantial changes in fire spread rates (Lloret et al. 2002; Ager et al. 2017). For instance, orchards and fruit trees played a key role in reducing fire spread since managed agricultural lands represent an effective barrier to restrict the surface fire spread.

A major zone with the highest values of FPI was identified in the southern part of the study area. This area was located in the provincial territory with the highest historical ignition point densities and the biggest fire size. High FPI values were also shown by the areas covered by fast-burning fuels, such as broad herbaceous pastures and cereal crops. The eastern part of the study area presented the lowest FPI values because of the low historical fire ignition densities and the small fire size (Fig. 6). These results may have direct and significant implications to target ignition prevention activities on the areas where the fires

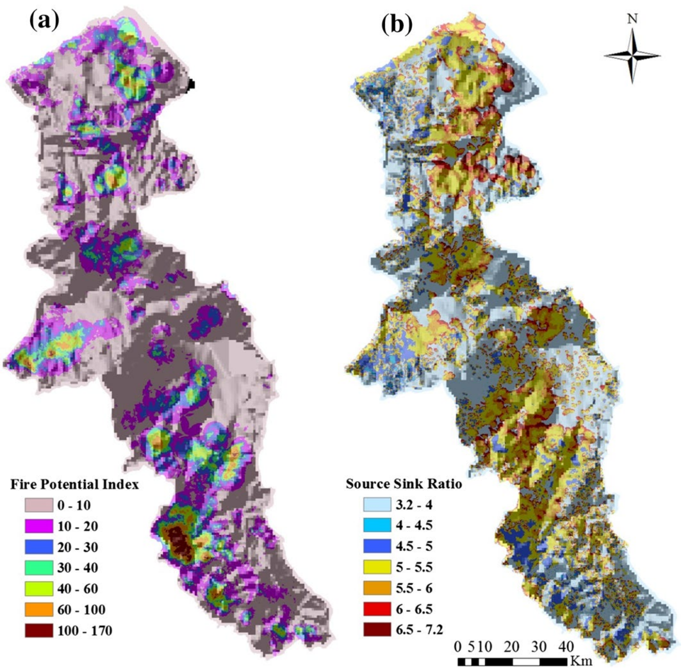

Fig. 6 Fire potential index (**a**) and Source sink ratio (**b**) maps of the study area

escaping from the initial attack may cause substantial losses in communities. Currently, ongoing wildfire management efforts in the study area include maintenance of tracks firebreaks, water points, and monitoring for early detection. Maintain firebreaks by reducing fuel loading are the main program that will reduce the intensity of a fire and therefore allow for more effectively combating and to also serve as a line from which a back burn can be started. Despite high fuel accumulations in some areas like plantations and prevailing drought conditions, there are no fuel management and prescribed burning programs underway. Quantitative risk assessment from this study can help local wildfire managers to prioritize preventive planning and investments in reducing ignitions.

According to SSR map (Fig. 6), the sink areas (low SSR) were mostly concentrated in the eastern part of the study area, which are covered by broadleaf forests (mainly Fagus and Quercus forests). On the contrary, wildfire sources (high SSR) were identified in the southern and northern parts of the area, predominantly covered by cereal crops and grazed pastures. Spatial variation in the source–sink ratio was pronounced and strongly affected by the continuity and arrangement of fuels. Pixels with small SSR values generated small fires relative to the probability of being burned by a fire originating elsewhere (Ager et al. 2012). The estimation of potential transmission of fire risk according to the SSR may suggest possible firefighting strategies, places that need vegetation management, areas that require more patrols and surveillance, and areas with increased fire intensity.

3.2 Wildfire exposure at fuels level

We analyzed the average values of the simulation outputs to characterize the fire exposure profiles among different vegetation types, municipalities, and weather scenarios. Scatterplots of average values for the outputs were also generated to illustrate the selected features with different fire risks (Figs. 7, 8, 9). The results showed significant differences in the modeled fire exposure factors in terms of both magnitude and spatial patterns. Broadleaf forests, conifer–broadleaf mix, and shrubby pastures presented the lowest values of BP and CFL (<0.0001 and <0.06 m, respectively). This can be explained by the presence of non-burnable fuels near the forests and the fragmented landscapes, especially in the east part of the province. A similar pattern in terms of fire severity was observed in deciduous

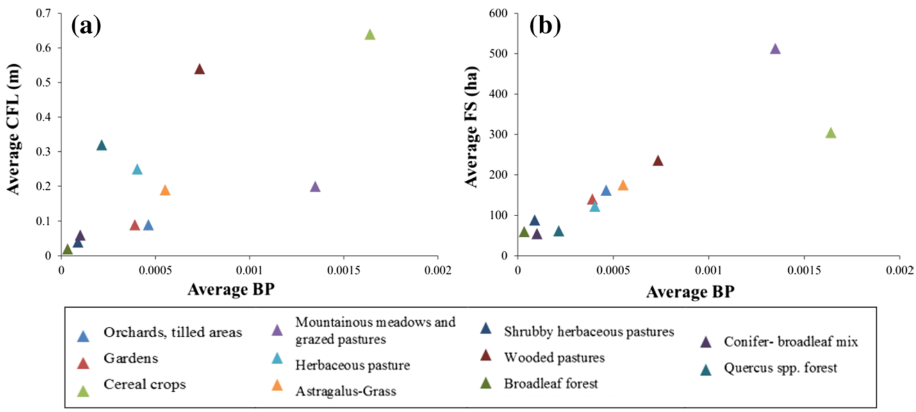

Fig. 7 Scatterplots of average conditional flame length vs. average burn probability (**a**) and average fire size vs. average burn probability (**b**) for each vegetation type of the study area

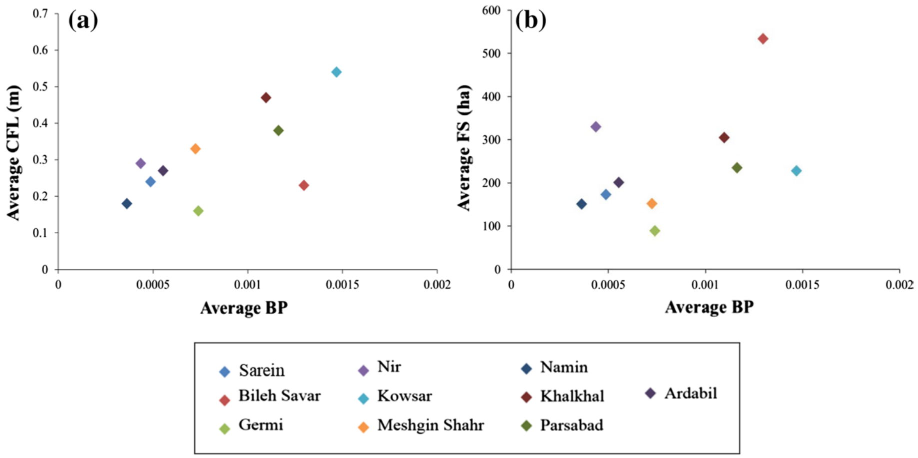

Fig. 8 Scatterplots of average conditional flame length vs. average burn probability (**a**) and average fire size vs. average burn probability (**b**) for each municipality in the study area

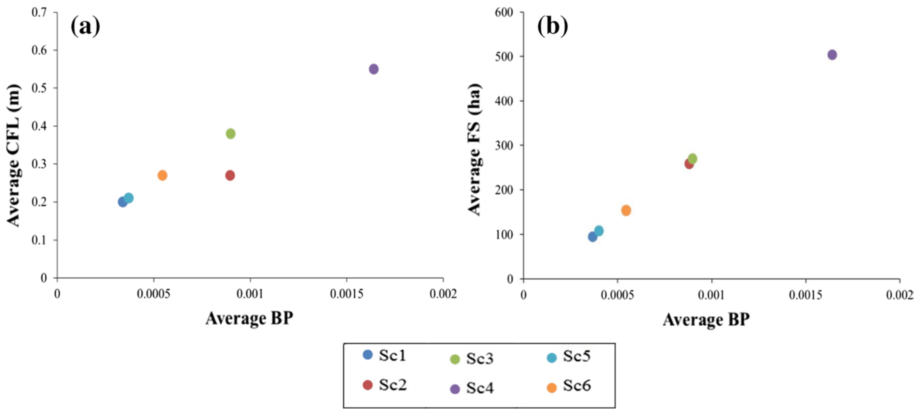

Fig. 9 Scatterplots of average conditional flame length vs. average burn probability (**a**) and average fire size vs. average burn probability (**b**) for each wind scenario in the study area

broadleaf forests and shrublands in fire-prone Eurasian boreal forests (Fang et al. 2018). The result is also consistent with observations in North America boreal forests where deciduous forests are found to be fire break and reduce landscape flammability owing to higher foliage moisture and less surface fuels (Rupp et al. 2002; Johnstone et al. 2011). Quercus spp. forest, herbaceous pastures, and Astragalus–Grass were identified to have very low hazard ($BP < 0.0005$ and $CFL < 0.4$ m). In these areas, intensive grazing reduces fire hazard through the reduction in surface fuel load. Diamond et al. (2009) and Weber et al. (2011) showed that livestock grazing in Idaho reduced grass biomass and cover, and ultimately fuel load, which resulted in reductions in fire intensity. In addition, in several regions it has been successfully used to assist grazing management and replace the clandestine use of fire by shepherds in high fire danger periods (Coughlan 2014). Gardens and orchards and tilled areas, which are often located in managed areas and have low fuel load, exhibited limited fire exposure, with BP smaller than 0.0005 and CFL less than 0.1 m on average. The result is consistent with the previous findings in a Mediterranean fire-prone area, where vineyards and orchards with the low presence of woods and shrubs in the surroundings, presented the average lowest values of CFL (Salis et al. 2013; Alcasena et al. 2015). Wooded pastures were characterized by a high CFL value (0.54 m), but presented low values of BP (0.0007) due to the low ignition probability on these areas. Simulation outputs for mountainous meadows and grazed pastures showed fairly high mean values of BP and low values of CFL. High BPs and CFLs were observed on cereal crops. The highest overall wildfire exposure was experienced by cereal crops and mountainous meadows areas with high fuel accumulation (BP > 0.001 and CFL > 0.6 m). These areas are overall characterized by a large number of fire events.

FS exhibited a strong spatial variability among and within the fuels. On average, FS exhibited a peak in mountainous meadows and grazed pastures (513 ha). FS was higher than 200 ha in cereal crops and wooded pastures. Orchards, tilled areas, gardens, herbaceous pastures, and Astragalus–grass presented average FS values between 100 and 200 ha. Shrubby pastures, broadleaf forest, conifer–broadleaf mix, and Quercus spp. forest showed lower values (FS < 100 ha).

3.3 Wildfire exposure at municipality level

For the creation of the other scatterplots, wildfire exposure was analyzed for the diverse municipalities of Ardabil Province (Fig. 8). The fire simulation outputs showed low values of fire exposure factors in the municipalities of Namin, Nir, Sarein, and Ardabil, compared with the other municipalities (BP < 0.001 and CFL < 0.5 m). Namin presented the smallest fire hazard, with BP and CFL values less than 0.0003 and 0.2 m, respectively. Meshgin Shahr and Germi exhibited low CFL (< 0.3 and < 0.2 m, respectively), with the same value of BP (0.0007). Khalkhal, Parsabad, and BileSavar have high fire hazard (BP > 0.001 and CFL > 0.2 m). In general, Khalkhal, Parsabad, Bilesavar, and Kowsar showed higher BP and a wide range of CFL values. Kowsar revealed the highest CFL (> 0.5 m) and BP greater than 0.0015. High wildfire exposure values in the municipalities are associated with a large amount of pastures, grasslands, and agriculture areas in Parsabad and BileSavar (northern part), and the high steepness and large presence of shrublands in Khalkhal and Kowsar (southern part).

In terms of FS, the results showed that some municipalities seemed to support large fire events (Table 4). The maximum average values were observed in BileSavar, Khalkhal, and Nir (> 300 ha). FS for Sarein, Kowsar, Meshgin Shahr, Namin, Parsabad, and Ardabil ranged from 100 to 300 ha. Germi had the lowest average FS among the municipalities (89 ha).

3.4 Effects of wind scenarios on wildfire exposure

Scatterplots showing the dispersal of BP-, CFL-, and FS-simulated values among the six wind scenarios illustrate a large range of variability (Fig. 9). The simulation results showed the variation in the values depending on the wind scenarios considered. Among the six scenarios, average BP and CFL varied from 0.00037 to 0.002 and from 0.2 to 0.55 m, respectively. The highest average BP and CFL among all wind scenarios were observed for southeast wind direction scenario (Sc4) (BP > 0.001 and CFL > 0.5 m). Dominant winds (Sc2 and Sc3) showed moderate high intensities (BP ~ 0.001 and CFL ~ 0.3 m). Sc1 and

Sc5 presented the lowest fire hazard (BP < 0.01 and CFL < 2 m). The simulation results in Sc6 presented relatively mild BP and CFL values (BP < 0.0004 and CFL < 0.2 m).

Average FS values ranged from 99 to 504 ha among the wind scenarios. On average, scenarios 1 and 5 showed the lowest FS (99 and 100 ha). The highest FS were observed in scenario 4 (504 ha).

4 Conclusions

Wildfires pose significant threat to people and property in northwestern Iran. Landscape-scale wildfire simulation modeling can be useful for analyzing potential wildfire risk and effects, evaluating historical changes and future trends in wildfire exposure, prioritizing management activities, as well as addressing and informing conservation, restoration, and risk management planning. The use of wildfire simulations in fire exposure assessment allows the mapping of burn probability and associated fire intensities in relation to key drivers including weather, fuel, topography, and spatial ignition patterns. The application of remote sensing methods can support mapping and characterization of some input data (i.e., fuel models and moisture) needed for wildfire spread modeling and thus further increase the potential of wildfire simulators for an integrated wildfire management strategy (Vilar et al. 2015; Kanga and Singh 2015).

We used MTT module in FlamMap v. 5 (Finney 2006) to simulate 60,000 fires considering historical weather scenarios. Simulation outputs highlighted that wildfire season dominant winds significantly affect fire likelihood. The statistical analysis also revealed significant differences among vegetation types and municipalities in terms of BP, CFL, and FS. Scatterplots of average patch values for simulation outputs helped in locating which of the studied features are in greater fire risk. Patterns of fuel types, together with wind direction and speed, were the main drivers of fire risk. The analysis will help the municipalities increase awareness and promotion of the social responsibility against wildfires risk, or plan to mitigate fire risk; and what municipalities are doing to build resilience in their communities.

Most of the budget in forestry is dedicated to fire suppression activities in fire management. Although fire suppression organization has been improved, the frequency of occurrence of high-intensity fires has been increasing recently. Climate change scenarios also indicate that wildfires are likely to further increase in number, size, and frequency. Socio-economic changes especially due to land use changes in the study area can foster the occurrence of the wildfire events. We implemented a fine-scale wildfire exposure analysis based on a fire modeling approach. Wildfire risk and exposure modeling can aid fire risk reduction management activities by identifying areas with high potential for forest fires and high risks to fire hazard, and those most vulnerable under extreme weather conditions.

The study demonstrates how the modeling approach can replicate historical wildfire exposure, and this approach can be replicated in other regions. We present the first application of fire spread modeling approach based on burn probability to analyze fire hazard and exposure at different levels in Iran and even at regional scale. The analysis outputs can have numerous applications in the study area, particularly to address the requirements of landscape managers to prioritize mitigation treatments and fire ignition prevention monitoring. However, further studies of fire risk methods in the field are necessary in order to validate and calibrate the outcomes of FlamMap MTT, especially in the vegetation conditions of the study area.

Acknowledgements This work was funded by the Research Project "Development of Wildland Fire Crisis management plan in Ardabil Province" and supported by the Vice-Chancellor for Research and Technology, University of Mohaghegh Ardabili, Ardabil, I. R. Iran.

References

Abatzoglou JT, Williams AP, Barbero R (2018) Global emergence of anthropogenic climate change in fire weather indices. Geogr Res Lett 46(1):326–336

Abdi O, Kamkar B, Shirvani Z, Teixeira da Silva JA, Buchroithner MF (2018) Spatial-statistical analysis of factors determining forest fires: a case study from Golestan, Northeast Iran. Geomat Nat Hazards Risk 9(1):267–280

Adab H, Kanniah KD, Solaiman K (2013) Modeling forest fire risk in the northeast of Iran using remote sensing and GIS techniques. Nat Hazards 65:1723–1743

Adab H, Atabati A, Oliveira S, Gheshlagh AM (2018) Assessing fire hazard potential and its main drivers in Mazandaran province, Iran: a data-driven approach. Environ Monit Assess 190:670

Ager AA, Finney MA, Kerns BK, Maffei H (2007) Modeling wildfire risk to northern spotted owl (*Strix occidentalis* caurina) habitat in Central Oregon USA. For Ecol Manage 246:45–56

Ager AA, Vaillant NM, Finney MA (2010) A comparison of landscape fuel treatment strategies to mitigate wildland fire risk in the urban interface and preserve old forest structure. For Ecol Manage 259:1556–1570

Ager AA, Vaillant NM, Finney MA (2011) Integrating fire behavior models and geospatial analysis for wildland fire risk assessment and fuel management planning. J Combust 2011:1–19

Ager AA, Vaillant NM, Finney MA, Preisler HK (2012) Analyzing wildfire exposure and source–sink relationships on a fire prone forest landscape. For Ecol Manage 267:271–283

Ager AA, Day MA, Finney MA, Vance-Borland K, Vaillant NM (2014) Analyzing the transmission of wildfire exposure on a fire-prone landscape in Oregon, USA. For Ecol Manage 334:377–390

Ager AA, Barros AMG, Preisler HK, Day MA, Spies TA, Bailey JD, Bolte JP (2017) Effects of accelerated wildfire on future fire regimes and implications for the United States federal fire policy. Ecol Soc 22(4):12

Ager AA, Houtman RM, Day MA, Ringo C, Palaiologou P (2019) Tradeoffs between US national forest harvest targets and fuel management to reduce wildfire transmission to the wildland urban interface. For Ecol Manage 434:99–109

Aghajani H, Fallah A, Fazlollah Emadian S (2014) Modelling and analyzing the surface fire behaviour in Hyrcanian forest of Iran. J For Sci 60:353–362

Alcasena FJ, Salis M, Vega-Garcia C (2015) A fire modeling approach to assess wildfire exposure of valued resources in central Navarra, Spain. Eur J For Res 135(1):87–107

Alcasena FJ, Salis M, Nauslarc NJ, Aguinaga AE, Vega-García C (2016) Quantifying economic losses from wildfires in black pine afforestations of northern Spain. For Policy Econ 73:153–167

Alcasena FJ, Salis M, Ager AA, Castell R, Vega-García C (2017) Assessing wildland fire risk transmission to communities in Northern Spain. Forests 8:30

Alcasena FJ, Ager AA, Pineda N, Vega-García C (2019) Towards a comprehensive wildfire management strategy for Mediterranean areas: framework development and implementation in Catalonia, Spain. J Environ Manage 231:303–320

Andela N, Morton DC, Giglio L, Randerson JT (2019) Global fire atlas with characteristics of individual fires, 2003–2016. ORNL DAAC, Oak Ridge, Tennessee, USA. https://doi.org/10.3334/ORNLDAAC/1642

Anderson HE (1982) Aids to determining fuel models for estimating fire behaviour. USDA Forest Service, Intermountain Forest and Range Experiment Station, General Technical Report INT-GTR-122 (Ogden, UT)

Arca B, Duce P, Laconi M, Pellizzaro G, Salis M, Spano D (2007) Evaluation of FARSITE simulator in Mediterranean maquis. Int J Wildland Fire 16:563–572

Arca B, Bacciu V, Pellizzaro G, Salis M, Ventura A, Duce P, Spano D, Brundu G (2009) Fuel model mapping by IKONOS imagery to support spatially explicit fire simulators. In '7th Int. Work. Adv. Remote Sens. GIS Appl. For. fire Manag. Towar. an Oper. use Remote Sens. For. fire Manag.', 2–5. (Matera)

Braun WJ, Jones BL, Lee JSW, Woodford DG, Wotton BM (2010) Forest fire risk assessment: an illustrative example from Ontario, Canada. J Probab Stat 2010:823018

Byram GM (1959) Combustion of forest fuels. In: Davis KP (ed) Forest fire control and use. McGraw-Hill Book Company, New York, pp 61–89

Calkin DE, Ager AA, Thompson MP (2011) A comparative risk assessment framework for wildland fire management: the 2010 cohesive strategy science report. General technical report RMRS-GTR-262. USDA Forest Service, Rocky Mountain Research Station, Fort Collins
Catchpole EA, de Mestre NJ, Gill AM (1982) Intensity of fire at its perimeter. Aust Forestry Res 12:47–54
Congalton RG (1991) A review of assessing the accuracy of classifications of remotely sensed data. Remote Sens Environ 37:35–46
Congalton RG, Green K (1999) Assessing the accuracy of remotely sensed data: principles and practices. Lewis Publishers, Boca Raton
Coughlan MR (2014) Farmers, flames, and forests: historical ecology of pastoral fire use and landscape change in the French Western Pyrenees, 1830–2011. For Ecol Manage 312:55–66
Davies KW, Boyd Chad S, Bates JD, Hulet A (2015) Winter grazing can reduce wildfire size, intensity and behaviour in a shrub-grassland. Int J Wildland Fire 25:191–199
Diamond JM, Call CA, Devoe N (2009) Effects of targeted cattle grazing on fire behavior of cheatgrass-dominated rangeland in the northern Great Basin, USA. Int J Wildland Fire 18:944–950
Dimitrakopoulos AP (2002) Mediterranean fuel models and potential fire behaviour in Greece. Int J Wildland Fire 11(2):127–130
Duff TJ, Cawson JG, Cirulis B, Nyman P, Sheridan GJ, Tolhurst KG (2018) Conditional performance evaluation: using wildfire observations for systematic fire simulator development. Forests 9:189
Dunn CJ, O'Connor CD, Abrams J, Thompson MP, Calkin DE, Johnston JD, Stratton R, Gilbertson-Day J (2020) Wildfire risk science facilitates adaptation of fire-prone social-ecological systems to the new fire reality. Environ Res Lett 15:025001
Eskandari S, Chuvieco E (2015) Fire danger assessment in Iran based on geospatial information. Int J Appl Earth Obs Geoinf 42:57–64
Eskandari S, Oladi Ghadikolaei J, Jalilvand H, Saradjian MR (2013) Detection of fire high-risk areas in northern forests of Iran using dong model. World Appl Sci J 27(6):770–773
Fairbrother A, Turnley JG (2005) Predicting risks of uncharacteristic wildfires: application of the risk assessment process. For Ecol Manage 211(1):28–35
Fang L, Yang J, White M, Liu Z (2018) Predicting potential fire severity using vegetation, topography and surface moisture availability in a Eurasian Boreal forest landscape. Forests 9:130
Faraji F, Alijanpour A, Sheidai Karkaj E, Motamedi J (2019) Effect of fire and rangeland banqueting on soil carbon sequestration in Atbatan summer rangelands, East Azerbaijan Province. ECOPERSIA 7(1):29–37
Fernandes PM, Loureiro C, Magalhães M, Pedro F, Fernandes M (2012) Fuel age, weather and burn probability in Portugal. Int J Wildland Fire 21:380–384
Finney MA (2002) Fire growth using minimum travel time methods. Can J For Res 32(8):1420–1424
Finney MA (2005) The challenge of quantitative risk analysis for wildland fire. For Ecol Manage 211:97–108
Finney MA (2006) An overview of FlamMap fire modeling capabilities. In: 'Fuels management—how to measure success: conference proceedings', 28–30 March, Portland, OR. (Comp PL Andrews, BW Butler), USDA Forest Service, Rocky Mountain Research Station Proceedings RMRS-P-41, pp 213–220
Finney MA, McHugh CWC, Grenfell ICI, Riley KL, Short KC (2011) A simulation of probabilistic wildfire risk components for the continental United States. Stoch Environ Res Risk Assess 25:973–1000
Haas JR, Calkin DE, Thompson MP (2013) A national approach for integrating wildfire simulation modeling into Wildland Urban Interface risk assessments within the United States. Landscape Urban Plann 119:44-53
Haas JR, Calkin DE, Thompson MP (2015) Wildfire risk transmission in the Colorado Front Range, USA. Risk Anal 35:226–240
Jaafari A, Mafi Gholami D, Zenner EK (2017) A Bayesian modeling of wildfire probability in the Zagros Mountains, Iran. Ecol Inform 39:32–44
Jaafari A, Razavi Termeh SV, Tien Bui D (2019) Genetic and firefly metaheuristic algorithms for an optimized neuro-fuzzy prediction modeling of wildfire probability. J Environ Manage 243:358–369
Jafarzadeh AA, Mahdavi A, Jafarzadeh H (2017) Evaluation of forest fire risk using the Apriori algorithm and fuzzy c-means clustering. J For Sci 63(8):370–380
Jahdi R, Darvishsefat AA, Etemad V, Mostafavi MA (2014) Wildfire spread simulation and wind effect on it (Case study: Siahkal Forest in Northern Iran). J Agricult Sci Technol 16:1109–1121
Jahdi R, Salis M, Darvishsefat AA, Mostafavi MA, Alcasena F, Etemad V, Lozano O, Spano D (2015) Calibration of FARSITE simulator in northern Iranian forests. Nat Hazards Earth Syst Sci 15:443–459
Jahdi R, Salis M, Darvishsefat AA, Alcasena F, Mostafavi MA, Etemad V, Lozano O, Spano D (2016) Evaluating fire modelling systems in recent wildfires of the Golestan National Park, Iran. Forestry 89(2):136–149

Johnstone JF, Rupp TS, Olson M, Verbyla D (2011) Modeling impacts of fire severity on successional trajectories and future fire behavior in Alaskan boreal forests. Landsc Ecol 26:487–500
Kalabokidis K, Palaiologou P, Finney M (2014) Fire behavior simulation in Mediterranean forests using the minimum travel time algorithm. In: Fourth fire behavior and fuels conference proceedings-at the crossroads: looking toward the future in a changing environment; 1–4 July 2013; St. Petersburg, Russia. International Association of Wildland Fire, Missoula, MT, pp 468–492
Kanga S, Singh SK (2015) Forest fire simulation modeling using remote sensing & GIS. Int J Adv Res Comput Sci 8(5):326–332
Legendre P, Legendre L (1998) Numerical ecology, 2nd edn. Elsevier, Amsterdam
Lloret F, Calvo E, Pons X, Díaz-Delgado R (2002) Wildfires and landscape patterns in the Eastern Iberian Peninsula. Landscape Ecol 17(8):745–759
Mahdavi A, Fallah Shamsi S, Nazari R (2012) Forests and rangelands' wildfire risk zoning using GIS and AHP techniques. Casp J Environ Sci 10:43–52
Mallinis G, Mitsopoulos I, Beltran E, Goldammer J (2016) Assessing wildfire risk in cultural heritage properties using high spatial and temporal resolution satellite imagery and spatially explicit fire simulations: the case of Holy Mount Athos, Greece. Forests 7:46
Massada AB, Radeloff VC, Stewart SI, Hawbaker TJ (2009) Wildfire risk in the wildland–urban interface: a simulation study in northwestern Wisconsin. For Ecol Manage 258:1990–1999
Miller C, Ager AA (2013) A review of recent advances in risk analysis for wildfire management. Int J Wildland Fire 22:1–14
Naghipour AA, Khajeddin SJ, Bashari H, Iravani M, Tahmasebi P (2015) The effects of fire on density, diversity and richness of soil seed bank in semi-arid rangelands of central Zagros region, Iran. J Biodivers Environ Sci: JBES 6(5):311–318
Oswald BP, Brouwer N, Willemsen E (2017) Initial development of surface fuel models for the Netherlands. For Res 6:207
Pahlavani P, Bigdeli B (2017) Providing the fire risk map in forest area using a geographically weighted regression model with Gaussian kernel and modis images, a case study: Golestan Province. Int Arch Photogramm Remote Sens Spat Inf Sci XLII-4/W4:477–481
Palaiologou P, Ager AA, Nielsen-Pincus M, Evers C, Kalabokidis K (2018) Using transboundary wildfire exposure assessments to improve fire management programs: a case study in Greece. Int J Wildland Fire 27:501–513
Palaiologou P, Ager AA, Evers C, Nielsen-Pincus M, Day M, Preisler HK (2019) Fine scale assessment of cross boundary wildfire events in the Western US. Nat Hazards Earth Syst Sci Discuss. https://doi.org/10.5194/nhess-2019-56
Parisien MA, Miller C, Ager AA, Finney MA (2010) Use of artificial landscapes to isolate controls on burn probability. Landsc Ecol 25:79–93
Parisien MA, Snetsinger S, Greenberg JA, Nelson CR, Schoennagel T, Dobrowski SZ, Moritz MA (2012) Spatial variability in wildfire probability across the western United States. Int J Wildland Fire 21:313–327
Parisien MA, Walker GR, Little JM, Simpson BN, Wang X, Perrakis DDB (2013) Considerations for modeling burn probability across landscapes with steep environmental gradients: an example from the Columbia Mountains, Canada. Nat Hazards 66:439–462
Parisien MA, Robinne FN, Perez JY, Denave B, DeLancey ER, Doche C (2018) Scénarios de probabilité et puissance potentielle des feux de végétation dans le département des Landes, France. Can J For Res 48(12):1587–1600
Parks SA, Parisien MA, Miller C (2012) Spatial bottom-up controls on fire likelihood vary across western North America. Ecosphere 3(1):1–20
Richards GD (1990) An elliptical growth model of forest fire fronts and its numerical solution. Int J Numer Meth Eng 30:1163–1179
Riley K, Thompson M (2017) An uncertainty analysis of wildfire modeling, Chap. 13. In: Riley Karin, Webley Peter, Thompson Matthew (eds) Natural hazard uncertainty assessment: modeling and decision support, geophysical monograph, vol 223, 1st edn. American Geophysical Union, Washington, pp 193–213
Rothermel RC (1983) How to predict the spread and intensity of forest and range fires. National Wildlife Coordinating Group, Boise
Rupp TS, Starfield AM, Chapin FS, Duffy P (2002) Modeling the impact of black spruce on the fire regime of Alaskan boreal forest. Clim Change 55:213–233
Sağlam B, Bilgili E, Küçük Ö, Durmaz BD (2008) Fire behavior in Mediterranean shrub species (Maquis). Afr J Biotechnol 7:4122–4129

Salis M, Ager AA, Arca B, Finney MA, Bacciu V, Duce P, Spano D (2013) Assessing exposure of human and ecological values to wildfire in Sardinia, Italy. Int J Wildland Fire 22:549–565
Salis M, Ager AA, Alcasena F, Arca B, Finney M, Pellizzaro G, Spano D (2015) Analyzing seasonal patterns of wildfire exposure factors in Sardinia, Italy. Environ Monit Assess 187:4175
Salis M, Arca B, Alcasena F, Arianoutsou M, Bacciu V, Duce P, Duguy B, Koutsias N, Mallinis G, Mitsopoulos I, Moreno JM, Pérez JR, Urbieta IR, Xystrakis F, Zavala G, Spano D (2016) Predicting wildfire spread and behaviour in Mediterranean landscapes. Int J Wildland Fire 25(10):1015–1032
Salis M, Del Giudice L, Arca B, Ager AA, Alcasena-Urdiroz F, Lozano O, Bacciu V, Spano D, Duce P (2018) Modeling the effects of different fuel treatment mosaics on wildfire spread and behavior in a Mediterranean agro-pastoral area. J Environ Manage 212:490–505
Salis M, Del Giudice L, Robichaud PR, Ager AA, Canu A, Duce P, Pellizzaro G, Ventura A, Alcasena-Urdiroz F, Spano D, Arca B (2019) Coupling burn probability and erosion models to quantify post-fire erosion before and after fuel treatments: a case study from Northern Sardinia, Italy. Int J Wildland Fire. https://doi.org/10.1071/WF19034
Scott JH (2007) Hazard. In: FireWords: Fire Science Glossary [electronic]. U. S. Department of Agriculture, Forest Service, Rocky Mountain Research Station, Fire Sciences Laboratory (Producer). Available: http://www.firewords.net
Scott JH, Burgan R (2005) Standard fire behavior fuel models: a comprehensive set for use with Rothermel's surface fire spread model. USDA Forest Service, Rocky Mountain Research Station, General technical report RMRS-GTR-153 (Fort Collins, CO)
Scott JH, Thompson MP, Calkin DE (2013) A wildfire risk assessment framework for land and resource management. General technical report. RMRS-GTR-315. U.S. Department of Agriculture, Forest Service, Rocky Mountain Research Station, 83 p
Sullivan AL (2009a) Wildland surface fire spread modelling, 1990–2007, 1: physical and quasi-physical models. Int J Wildland Fire 18:349–368
Sullivan AL (2009b) Wildland surface fire spread modelling, 1990–2007, 2: empirical and quasi-empirical models. Int J Wildland Fire 18:369–386
Sullivan AL (2009c) Wildland surface fire spread modelling, 1990–2007, 3: simulation and mathematical analogue models. Int J Wildland Fire 18:387–403
Thompson MP, Calkin DE (2011) Uncertainty and risk in wildland fire management: a review. J Environ Manag 92(8):1895–1909
Thompson M, Calkin D, Finney M, Ager A, Gilbertson-Day J (2011) Integrated national-scale assessment of wildfire risk to human and ecological values. Stoch Environ Res Risk Assess 25:761–780
Thompson MP, Scott J, Langowski PG, Gilbertson-Day JW, Haas JR, Bowne EL (2013) Assessing watershed-wildfire risks on national forest system lands in the Rocky Mountain Region of the United States. Water 5:945–971
Thompson MP, Phil B, April B, Scott JH, Julie GD, Alan T, Jennifer A, Haas JR (2016) Application of wildfire risk assessment results to wildfire response planning in the southern Sierra Nevada, California, USA. Forests 7(3):64
Vilar L, Camia A, Ayanz JSM (2015) A comparison of remote sensing products and forest fire statistics for improving fire information in Mediterranean Europe. Eur J Remote Sens 48:345–364
Weber KT, McMahan B, Russell G (2011) Effect of livestock grazing and fire history on fuel load in sagebrush-steppe rangelands. In: Wildfire effects on rangeland ecosystems and livestock grazing in Idaho. http://giscenter.isu.edu/research/techpg/nasa_wildfire/template.htm
Zha S, Zhang S, Cheng T, Jianmin Chen J, Huang G, Li Z, Wang Q (2013) Agricultural fires and their potential impacts on regional air quality over China. Aerosol Air Qual Res 13:992–1001